Available online at www.sciencedirect.com
ScienceDirect
Journal of Molecular Catalysis A: Chemical 258 (2006) 203–215
JOURNAL OF MOLECULAR CATALYSIS A: CHEMICAL
www.elsevier.com/locate/molcata

DFT studies of methanol decomposition on Ni(1 0 0) surface: Compared with Ni(1 1 1) surface

Yu-Hua Zhou [a], Pei-Hong Lv [b], Gui-Chang Wang [a,*]

[a] *Department of Chemistry, Center of Theoretical Chemistry Study, Nankai University, Tianjin 300071, PR China*
[b] *Department of Chemistry, An Yang Normal College, An Yang 455000, PR China*

Received 17 December 2005; received in revised form 29 March 2006; accepted 1 April 2006
Available online 11 July 2006

Abstract

The decomposition of methanol on Ni(1 0 0) surface has been investigated using DFT-GGA (density functional theory-generalized gradient approximation) method with the repeated slab models, and compared in detail with that on Ni(1 1 1) surface. The adsorption energies as well as the adsorbed structure for the possible adsorbed species involved in this reaction were obtained and compare to that on Ni(1 1 1). For the reaction path calculation, the DFT-GGA results showed that both of the C–H bond and O–H bond broken are the favorable reaction paths on Ni(1 0 0), which is different from the case of Ni(1 1 1) in which only the O–H bond broken is the perfected reaction path, suggesting methanol decomposition reaction may be a structure-sensitive reaction. It was also found that the rate-limiting step (RLS) is the abstraction of hydrogen from methoxy for the O–H bond broken pathways, and it is similar to the case of Ni(1 1 1).
© 2006 Published by Elsevier B.V.

Keywords: Methanol decomposition; Ni(1 0 0); Kinetics mechanism; Structure-sensitive; DFT calculation; Slab model

1. Introduction

Understanding and controlling the physical and chemical mechanisms behind reactions in heterogeneous catalysis stand as one of the long-term goals for surface science, and also, a sound understanding of the chemical reaction is a fundamental aim of chemistry. In particular, the reaction of methanol on metal surfaces is a catalytically important reaction. By studying this reaction one can enhance the understanding of CH_3OH-based catalysis [1], and provide insight into the fundamental of bond making/breaking involved, which will contribute to a better understanding of carbon monoxide hydrogenation and methanol synthesis. Furthermore, the decomposition reaction of methanol itself is currently attracting widespread attention due to possible usage of methanol as a hydrogen source in fuel cell application.

Therefore, there has been a growing interest in the experimental and theoretical studies relating to methanol reactions on a variety of transition metal surfaces. Many surface science techniques have been employed, including STM on Cu(1 1 0) [2], UPS on Ni foil [3], TPEELS on Ni(1 1 0) [4], XPS, SIMS on Pd(1 1 1) [5], IRAS on Pt(1 1 1) [6], EELS on Ru(0 0 0 1) [7], HREELS and TPRS on Fe(1 0 0) [8], and so on. As on Ni(1 0 0) metal surface, the adsorption and decomposition of methanol, CH_3OH, has also been previously studied by means of conventional techniques [9–14], which suggested that for Raney nickel catalysts the low indexed surface planes as (1 0 0) are the catalytically more active surface [15]. A number of previous investigations have demonstrated that methanol adsorbed multilayers without dissociation at a surface temperature of 100 K for high exposures. When the surface is heated, little methanol desorbs. Instead, it decomposes to the adsorbed methoxy intermediate at roughly 250 K, and followed by the successive dehydrogenation to CO and H. The TPR and FTIR analysis [16,17] indicate that methanol decomposes exclusively via a methoxy intermediate initial with the scission of the O–H bond from 140 to 240 K on nickel surface, and then methoxy decomposes to adsorbed carbon monoxide and hydrogen at 240–290 K. Indeed, the CH_3O(a) species has been stabilized on nickel at 180 K [11,18–23], and the electron energy loss spectroscopy (EELS) [11], scanning kinetic spectroscopy (SKS) [18], time-resolved-EELS (TR-EELS) [4,19], optical second harmonic generation (SHG) [20], reflection adsorption infrared

* Corresponding author. Tel.: +86 22 23505244; fax: +86 22 23502458.
E-mail address: wangguichang@nankai.edu.cn (G.-C. Wang).

1381-1169/$ – see front matter © 2006 Published by Elsevier B.V.
doi:10.1016/j.molcata.2006.04.013

spectroscopy (RAIRS) and kinetic isotope effect (KIE) [21] have all shown that methoxy species are stable up to 290 K. Related experiments also report that CH_3O on nickel is known to decompose near or above 300 K [11,23]. FTIR analysis [17] of the symmetry vibrational modes suggests that methoxy bind normal to the Ni(1 0 0) surface at fourfold hollow sites and bridge site with C_s symmetry, at least at low coverage. The methoxy species may either recombine with adsorbed H, thus desorb as methanol [18] or further decompose to H(a) and CO(a) which eventually desorb as H_2 ($T > 300$ K) and CO ($T > 400$ K). This is in contrast with the higher stability of methoxy groups on oxygen precoveraged silver and copper surface, where occurs the decomposition to formaldehyde and hydrogen [24–28].

A complete mechanistic study of surface reactions can be best accomplished with the knowledge of the identification of the stable surface intermediates under investigation and the desorbing gaseous products. The methoxy fragment has been postulated to be a key intermediate in a number of heterogeneous catalytic processes involving methanol as either a reactant or product, and it has been investigated many times both experimentally and theoretically [26,29–39]. On Ni(1 0 0), a quasi-stable COH [40] or HCO [41] intermediate has also been proposed using IR and temperature-programmed reaction spectroscopy, respectively, but more recent publications [14,42,43] did not observe such species. Friedrich suggested that a lifetime of only a few milliseconds together with the difference in applied probing techniques may result in few investigators finding them [44], indicating that intermediates are less stable and decompose rapidly compared with the methoxy in the whole methanol decomposition process. Thus the adsorption of other intermediates (HCO, H_2CO, etc.) have been investigated mostly through theoretical methods, such as many-electron embedding theory, extended Hückel calculations, generalized valence-bond (GVB) and B3LYP-DFT method [45–48].

On the other hand, in connection with a particular reaction, rational designing of new catalysts requires knowledge of the elementary mechanisms, the adsorption modes of the mediate species, and the nature of the preferred adsorption sites. There are some literatures of theoretical studies related to methanol decomposition and the meditate species [49–55], however, there seems to be a matter of controversy about the reaction mechanism. An important issue concerns whether the first step of methanol decomposition occurs via an O–H bond scission [51,52], or a C–O bond scission [56–59] or a C–H bond scission [54,60,61], in which the scissions lead to the formation of methoxy (CH_3O), methyl (CH_3) and hydroxyl (OH), and hydroxymethyl (CH_2OH), respectively.

Density functional theory (DFT) method [62–64] has been helpful and providing a clear indication as to how these catalytic reactions are likely to take place owing to advances in computational speed, along with the development of new algorithms. And the results can complement the results of experimental investigations for stable adsorbed species. For example, these calculations can be used to predict the energetics of highly reactive intermediates and transition states that cannot be observed experimentally [65]. Aiming to understand the mechanisms behind the methanol decomposition, in the present paper, we carry out the periodic DFT calculations to probe microscopic decomposition pathways and the surface intermediates that may be formed on Ni(1 0 0) via the cleavage of O–H, C–O, C–H bonds. That is, we investigate some pivotal transition state, the corresponding adsorbed intermediates, in order to identify and compare the most favorable pathways during methanol decomposition on Ni-base catalyses. The DFT calculations in the present work is an extension of the work reported previously for methanol decomposition on Ni(1 1 1) [66,67], and by comparing with it we further investigate whether exists the structure-sensitive in the adsorption energy and the reaction barrier energy.

2. Calculation method and model

Self-consistent periodic calculations based on density functional theory, with the PBE generalized gradient approximation for the exchange and correlation energy calculation corrected, were conducted for three-layer Ni(1 0 0) slabs. The $p(3 \times 2)$ three-layer unit cell was repeated periodically, which means a coverage of only 1/6 ML monolayer for a single adsorbate on the surface, and separated by about 10 Å of vacuum between two successive metal slabs. Total energy calculations were performed using a package STATE [68–71] (Simulation Tool for Atom TEchnology) which has been successfully applied to adsorption problems. Ion cores are treated by Troullier–Martions type norm-conserving pseudo-potential [72] and valence wave functions are expended by a plane wave basis set with the cut-off energy of 25 Ry. In calculations, a Monkhorst–Pack mesh of $4 \times 6 \times 1$ special k-point sampling in the surface Brillouin zone was used [52,53,60]. The substrate atoms held fixed in their bulk crystal configuration, while the adsorbates were allowed to relax all degrees of freedom for optimization until the 'max force' on each atom was smaller than 0.001 hattree/Borh. Therefore, the unrelaxed model is employed here, and the adsorbates are placed on only one side of the two slab surfaces.

A path connecting the initial and final states is the minimum energy path (MEP). The maxima on the MEP are the different saddle points on the potential energy surface, and the highest saddle point relative to that of the initial state gives the activation barrier of the reaction, and determines the overall rate. The nudged elastic band (NEB) method is an efficient method for finding the MEP between the given initial and final state [73–75]. This method consists of making a chain composed of a set of images between the structures corresponding to the reactants and the products of the considered reaction. The initial image configurations of reaction paths are generated from a linear interpolation between the initial state and the final state. An interaction between the adjacent images is added to ensure the continuity of the path, and the essential feature of the forces on the images does not interfere with the convergence of the elastic band to the MEP, as well as ensure the distribution of images along the MEP. Here, the highest point along the MEP is considered as the transition state along the chosen reaction path. In order to locate the highest saddle (i.e., the transition state), we use a more effective NEB method or more exactly, the modified NEB method, that is, the adaptive nudged elastic

band (ANEBA) method [76]. It has been shown to give many excellent convergences to the saddle points [60,52,53,77,78].

Although the effect of spin polarization appears in general in the adsorption energies [66], the geometrical properties are remarkably well reproduced by the nonmagnetic calculations. As an example for CH_3O adsorption on Ni(1 1 1) [66], the C–O bond being shortened by only 0.005 Å, the distance of C atom to the metal surface being extended by 0.074 Å, and the binding energy is only reduced by 10 kJ/mol. The effect of the surface relaxation has been both investigated in our previous work [79], we find that the binding energy of methoxy for relaxed model is −257.6 kJ/mol and the configuration parameters on surface layer relaxed model are also very similar to the unrelaxed model. And the effect of spin polarization brings it to −239.9 kJ/mol. Therefore, these two factors affect binding energy oppositely, and it is not surprising that we find the marvelous similarity on adsorption energy of 245.0 kJ/mol (comparing with 249.6 kJ/mol) when including both effects of magnetization and relaxation. As considering the effect on activation energy of spin polarization and relaxation, we have checked up the rate-limiting step of methanol decomposition on Ni(1 1 1) surface, the methoxy dehydrogenation, and find that the energy barrier is only raised by 7 kJ/mol [66]. So, for reducing the computational costs, all calculations about the intermediates and the reaction path in this work are performed without spin polarization and surface relaxation. Considering the difference of (1 1 1) and (1 0 0), however, we also test the effect of spin polarization and the surface-relaxation on the activation energy for the rate-limiting step in the present work.

The adsorption energy (or Binding energy), E_{ads}, is calculated as the energy difference:

$$E_{ads} = E_A + E_M - E_{A/M}$$

where $E_{A/M}$ is the total energy of the system of adsorbate A on metal surface M, and E_A and E_M are the total energies of the isolated adsorbate and metal surface, respectively.

3. Results and discussions

Experimentally, it is generally accepted that methanol decomposition involves the adsorption of CH_3OH and its successive dehydrogenation, yielding linearly bonded CO on Ni(1 0 0) surface [9–14]. While theoretical calculations have proved that there are three kinds of bond scissions involved in the first step of its decomposition. Considering that the reaction pathway of molecule dissociation may be involve the adsorption on surface, the possible elementary reactions of the methanol decomposition are summarized as follows, some of them, excluding those asterisked steps which will be investigated in the future, will be discussed in detail later:

$$CH_3OH(g) \rightarrow CH_3OH(a) \quad (M1)$$

$$CH_3OH(a) \rightarrow CH_3O(a) + H(a) \quad (M2)$$

$$CH_3OH(a) \rightarrow CH_2OH(a) + H(a) \quad (M3)$$

$$CH_3OH(a) \rightarrow CH_3(a) + OH(a) \quad (M4)$$

$$CH_3O(a) \rightarrow H_2CO(a) + H(a) \quad (M5)$$

$$xH_2CO(a) \rightarrow (H_2CO)_x(a) \quad (M6^*)$$

$$H_2CO(a) \rightarrow HCO(a) + H(a) \quad (M7)$$

$$HCO(a) \rightarrow CO(a) + H(a) \quad (M8^*)$$

$$CH_2OH(a) \rightarrow H_2CO(a) + H(a) \quad (M9^*)$$

$$CH_2OH(a) \rightarrow CHOH(a) + H(a) \quad (M10^*)$$

$$CHOH(a) \rightarrow COH(a) + H(a) \quad (M11^*)$$

$$COH(a) \rightarrow CO(a) + H(a) \quad (M12^*)$$

$$CHOH(a) \rightarrow HCO(a) + H(a) \quad (M13^*)$$

where (a) and (g) indicate being adsorbed on a surface and in gas state, respectively.

The adsorption of small molecule and radical at metal surfaces is of considerable experimental as well as theoretical interest since they are present as the reaction products or intermediates in heterogeneous catalytic process. However, the adsorption energy of species corresponding to methanol decomposition has few been experimentally measured, since it is difficult to determine and requires very accurate calorimetric measurement. A theoretical approach based on the first principle DFT calculations is therefore useful, and the calculated structural parameters and energies will be compared with the available experimental data.

3.1. Adsorption energies and geometry of possible intermediate fragments

The Ni(1 0 0) surface is more open than Ni(1 1 1), which exhibits three high-symmetry adsorption sites: top, bridge, and fourfold hollow sites, shown in Fig. 1. While Ni(1 1 1) exhibits top, bridge and threefold hollow sites. Table 1 summarizes the most important information of the adsorption geometry parameters and the E_{ads} for all related species adsorbed at the most stable site on the unrelaxed slab model of Ni(1 0 0), and the E_{ads} on Ni(1 1 1) are also listed for comparison. It is noticed that the slab model is preferred to obtain energetics of the surface species, since this approach rigorously accounts for the true electronic structure and extended field effect for well-defined surface. Compared with slab model, the energetics predicted from the cluster approach may depend on the cluster size and shape, although the predicted structures of the adsorbates still

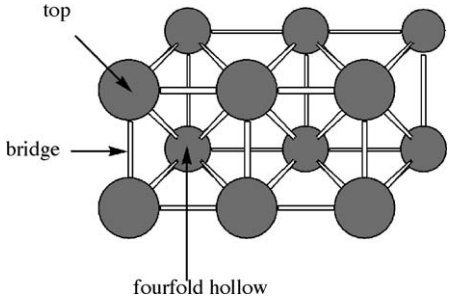

Fig. 1. Section of the Ni(1 0 0) surface. The arrows indicate the position of the three high-symmetry sites.

Table 1
Properties of methanol decomposition intermediates on Ni(1 0 0)

Species	Site	$R(\perp)$[a]	R(CO)	≠(CONi)	≠(OCNi)	R(ONi)	R(CNi)	Binding energy (kJ/mol)	Bonging energy (kJ/mol)[b]
CH_3OH	Top	2.192	1.445	142.9		2.207		−25.48 −32.13	−16.26
CH_3O	Fourfold Bridge	1.139	1.464	122.9		2.097		−260.26 −239	−249.64
CH_2OH	Top	1.860	1.471		109.9		1.925	−176.98	−162.19
H_2CO	η^2	1.409	1.410	102.7	109.3	1.922	1.979	−149.81	−99.55
HCO	η^2	1.287	1.370	100.2	113.8	1.940	1.910	−303.68	−232.17
CO	Fourfold Bridge Top	1.043	1.227		120.6		2.047	−218.54 −208.12 −176.02	−223.60
H	Fourfold	0.596						−273.43	−284.32
CH_3	Twofold Top	1.641					2.062	−184.14 −169.00	−196.97
OH	Fourfold Bridge	1.125				2.090		−324.54 −298.10	−307.77

[a] All distances in angstroms, angles in degree, and energies unit in kJ/mol.
[b] The binding energy on Ni(1 1 1).

appear to be in good agreement with the available experimental data and with the more rigorous slab approach. The advantages of slab model will be embodied when comparing with the available experimental conclusions in later sections.

The physical origin of the adsorbate–nickel bonding will be interpreted on the basis of the Anderson–Newns model [80], which suggested that the adsorbate–metal bonding is achieved via two steps: the adsorbate frontier orbitals interact with the metal sp states, leading to a shifted and broadening frontier orbitals. Second, the broadening frontier orbitals further mix with the narrow and localized metal d states to give rise to a deep-lying filled bonding state and an anti-bonding state. And we will also interprete the difference of bonding between Ni(1 0 0) and Ni(1 1 1) by their surface configuration.

3.1.1. Adsorbed methanol

DFT calculations show that the molecule attaches via the oxygen atom with the O–C axis tilted 37.1° (Fig. 2), which is consistent with both theoretical and experimental indication that the on-top site is a more favorable position for the adsorption of CH_3OH. Including the observation of SFG technique, experiment indicates that methanol is bound to the surface with the O–C bond tilted $25 \pm 10°$ from the surface normal, and suggests that this tilting is consistent with the bonding angle expectation if methanol is bound to the surface via the oxygen lone pair orbital [43]. The calculated E_{ads} of methanol, 25.48 kJ/mol, is in agreement with the new modified molecular beam relaxation spectrometry (MBRS) results, which show an adsorption energy of 22.4 kJ/mol on polycrystalline Ni [44]. This small adsorption energy is indicated by a rather long Ni–O bond length (2.207 Å) in the optimized structure, as shown in Fig. 1, and so well agrees with the above experimental conclusion that methanol is adsorbed on nickel surfaces molecularly under UHV conditions at low temperatures. The preferred adsorption site and the structural parameters of methanol adsorption on Ni(1 0 0) are very similar to Ni(1 1 1) surface [66] except that the distances of the molecule to the metal surface, i.e., the oxygen atom to the nickel atom are slightly shortened, due to the more openness of (1 0 0), then forming the higher adsorption energy than on Ni(1 1 1). More interestingly we find that methanol molecule is keeping σ_v mirror plane symmetry as in gas phase on both crystal surfaces, which also reflects the weak interaction. Moreover, Greeley and Mavrikakis [52,54] also found that methanol binds through oxygen at a top site on Pt(1 1 1), Hu and co-workers [51] found methanol atop the Pd(1 1 1) surface by using DFT-GGA method through slab model, and both were reported almost the same adsorption geometry as here.

3.1.2. Adsorbed methoxy

For the adsorption of methoxy on the Ni(1 0 0) surface (Fig. 2), the optimized configuration is that, through oxygen in fourfold hollow site with the C–O bond perpendicular to the Ni(1 0 0) surface, the CH_3O group maintains its local C_{3v} symmetry and the three hydrogen atoms keep in a plane paralleling to the metal surface. Hence, the direct interaction of the methyl group with the nickel surface is found to be weak. It is identical to the FTIR study on the symmetry of the model [17], which suggests that methoxy binds normal to the surface both in fourfold hollow site and bridge site with C_s symmetry, at least at low coverage. Normal or near normal orientation of the molecular axis of the CH_3O radical is also found on the Ni(1 1 1) surface through the early HREELS, the very recent FTIR, and the ultraviolet photoemission studies [11,22,33]. The calculated length of C–O bond, 1.464 Å, for CH_3O adsorbed on Ni(1 0 0) is in good agreement with the results of our previous work on Ni(1 1 1) [66], 1.444 Å. Although the O–Ni distance on Ni(1 0 0) is longer than on Ni(1 1 1), the more diffusive orbital of O 2p lone pair electrons in methoxy is responsible for the surface bonding, and

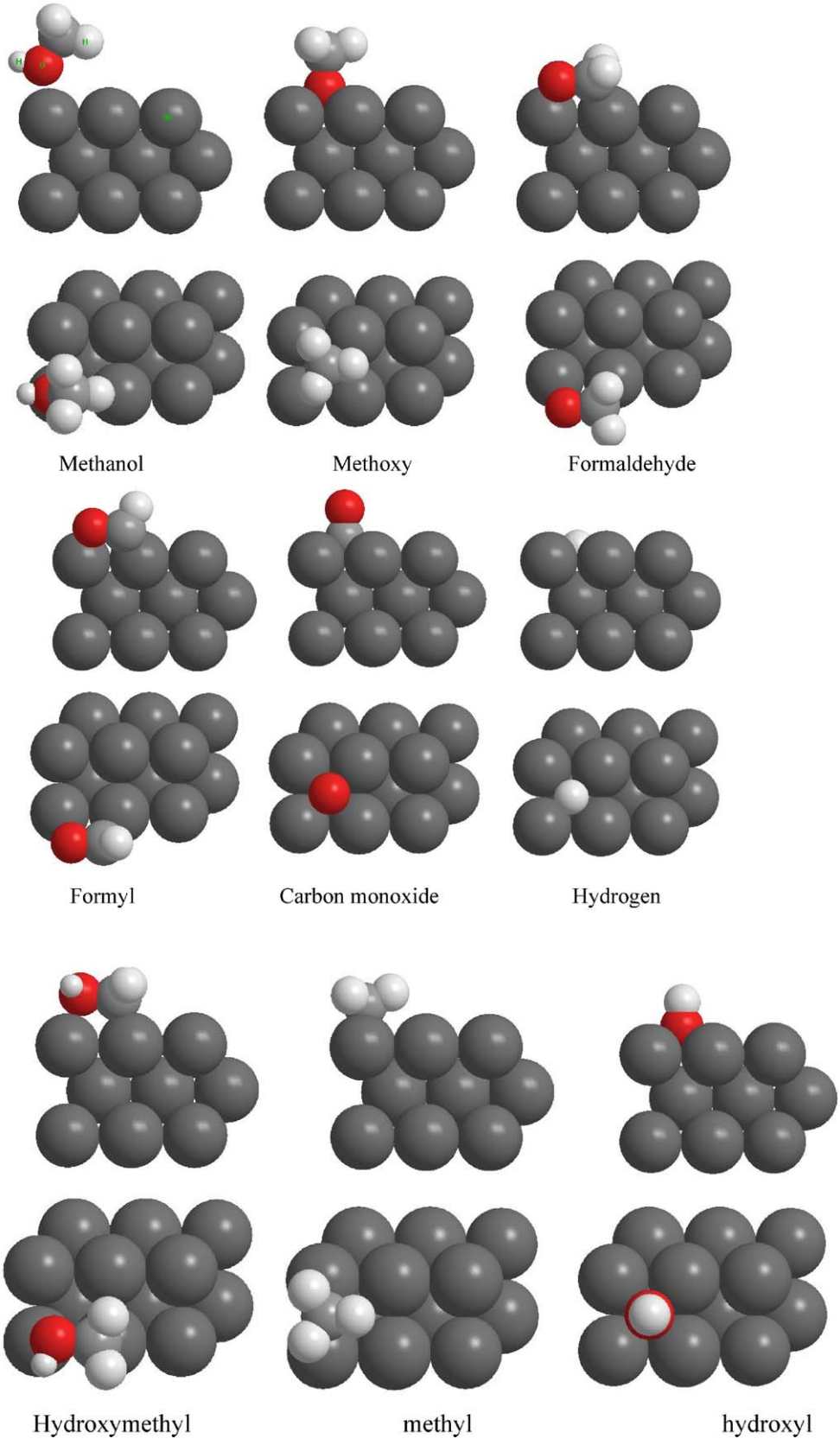

Fig. 2. The most stable binding configurations for all the possible intermediates in the methanol decomposition.

still forming a stronger adsorption on Ni(1 0 0). The calculated adsorption energy is 260.26 kJ/mol, again slightly higher than that of Ni(1 1 1) surface. In general, the more open the surface, the lower the coordination member, and the higher the adsorption energy. When the surface is more open, the surface atoms have fewer nearest neighbors, and the surface atoms should be more coordinatively unsaturated than those atoms with more nearest neighbors. The lower coordination number of metal atoms on Ni(1 0 0) surface, 8 versus 9 on Ni(1 1 1), should lead to a stronger back-bonding as compared with Ni(1 1 1), and hence a somewhat higher adsorption energy. However, this principle is not universal, because other factors such as the type of site of adsorption, the change of adsorption configuration, and the steric effect may be important.

By the way, Madix and co-workers also calculated the methoxy on Ni(1 0 0) using an ab initio embedding theory and found it oriented with its C–O bond tilting 5° [31] at a fourfold sited, corresponding to a 384 kJ/mol adsorption energy. This discrepancy with ours may be due to the model effect and the computational methodology (slab versus cluster; DFT versus many-electron theory).

3.1.3. Adsorbed formaldehyde

Aldehydes have been proposed as important intermediates during alcohol synthesis on supported transition metal catalysts. Formaldehyde can be adsorbed on metal surfaces through two type of configurations, i.e., with the oxygen lone pair electrons in an upright η^1(O) configuration, or in an η^2(C, O) configuration where both the carbonyl carbon and oxygen atoms interact with the surface metal atoms. Few experimental data exist for the adsorption of formaldehyde on nickel because it easily decomposes or polymerises [36]. Barteau and co-workers have examined the adsorption of aldehyde on group VIII metal surfaces [35,81–84]. Their analysis suggest that the preferred mode is the η^2 configuration, and conclude that the formaldehyde binds to the surface through the carbonyl π orbital and simultaneously through overlap between the metal d state and the carbonyl π^* orbital. This type of back-bonding strengthens the metal–aldehyde bond and reduces the C–O bond order of the adsorbed aldehyde, indicated by a much longer C–O bond (1.410 Å in this work) than the gas phase value of 1.22 Å, releasing the high adsorption energy of 149.81 kJ/mol. In the optimized structure, as shown in Fig. 2, formaldehyde prefers to bind in the η^2 configuration, the carbonyl group of formaldehyde is oriented parallel to the metal surface such that the Ni–C and Ni–O bonds formed are of nearly the same lengths (1.979 and 1.922 Å, respectively), while the hydrogen atoms are directed away from the surface. It is noticed that, although the optimized geometries of H_2CO molecule on Ni(1 1 1) and Ni(1 0 0) seem very similar [66], there are differences, the R_{CNi} and R_{ONi} are 1.979, 1.922 Å for Ni(1 0 0), and 1.938, 1.964 Å for Ni(1 1 1), respectively. Considering the bonding ability of carbonyl π orbital is much stronger at the O atom end, the adsorption energy is much small on Ni(1 1 1) for the longer R_{ONi}. And both adsorptions are significantly stronger than molecular chemisorption, such as the case of methanol discussed above. However, by comparing the differences in the ∠CONi, ∠OCNi on the (1 0 0) (102.7°, 109.3°) and those on the (1 1 1) (102.1°, 109.3°), we may have reason to believe that the configuration of (1 1 1) is associated with a local minimum.

3.1.4. Adsorbed formyl

There are three possible types of surface formyl, namely η^2(C, O), η^1(C) and η^1(O), i.e., bonding to the surface via both C and O atoms, via the C atom, and via the O atom, respectively. In this paper, we only describe the adsorption of HCO at η^2 bridge site, as shown in Fig. 2. The calculated C–H and C–O bond lengths at the optimized configuration are 1.106 and 1.376 Å, respectively, with the adsorption energy of 303.68 kJ/mol and the H–C–O angle of 112.3°. Previous ab initio configuration interaction (CI) level calculations showed that formyl had essentially the same adsorption energy at atop, bridge and fourfold sites via C atom bonding to surface, namely 265.43 kJ/mol, and the C–O bond was parallel to the surface for fourfold and bridge sites by using a many-electron embedding theory [45]. Also, since the coordination number here is two (η^2) and that in Ni(1 1 1) is one (η^1), it is reasonable to have the adsorption energy on Ni(1 0 0) is higher than that on Ni(1 1 1) (Table 1).

3.1.5. Adsorbed carbon monoxide

There are many experimental and theoretical studies [63,85–87] of interaction between CO and transition metal surfaces because of the potential usage of Fischer–Tropsch chemistry in the production of hydrocarbons and synthetic alcohol fuels. Carbon monoxide adsorbs molecularly on Ni(1 0 0) surface and has been studied using infrared reflection-adsorption spectroscopy (IRAS), low energy electron diffraction (LEED) [85], static and time-resolved Fourier transform infrared spectroscopic and threshold temperature-programmed desorption (TTPD) [88], suggesting it adsorbs onto atop and bridge sites. While Madix et al. find it is adsorbed onto fourfold hollow site by temperature-programmed reaction spectroscopy [12], and the desorption kinetic parameter, E_d, is found to be 128 ± 2 kJ/mol at coverage of 0.21 ML through the TTPD analysis [89]. Tardy and co-workers obtain a 125 kJ/mol adsorption energy by vibrational electron energy loss spectroscopy (EELS) [90]. The adsorption energy are both a little lower than our calculated values of 176.02, 208.12, and 218.54 kJ/mol for CO adsorbed on atop, bridge, and fourfold sites at 1/6 ML, respectively. From theoretical point of view, Hammer [87] reports the adsorption energy of 185 kJ/mol through DFT-PBE with the spin polarized calculations at fourfold hollow site, which is slightly less than ours. This discrepancy may be due to the spin effect, the higher coverage used in their calculations (1/4 ML versus 1/6 ML in our work), or to both. In the top view of CO adsorption geometry in Fig. 2, the CO molecule is found to be normal to the Ni(1 0 0) surface with the C–O molecular axis of 1.227 Å and Ni–C bond of 2.047 Å, while on Ni(1 1 1) [66] they are 1.208 and 1.942 Å. The longer C–Ni bond on Ni(1 0 0), which is formed by a less diffusive 5σ orbital of CO (comparing with the O 2p in methoxy, indicates it is a little weaker than on Ni(1 1 1), which is consistent with the experimental results [91] on binding energies, −125 and −117 kJ/mol on Ni(1 1 1) and

Ni(1 0 0), respectively, although the coordination number is 4 on Ni(1 0 0) and 3 on Ni(1 1 1). Therefore, the increasing coordination number of adsorption site may play a counteractant role: the bonding between CO molecule and the four nearest metal atoms could not be formed very well, comparing to bonding with three nearest on Ni(1 1 1). From the CO bonding model of Hammer [87] based on the Anderson–Newns model, the weaker bonding of CO on Ni(1 0 0) is in complete agreement with the theoretical interpretations developed by Blyholder [92] and others [86], that is, the language of electron donation from the CO 5σ orbital to the metal and the back donation from the metal to the CO $2\pi^*$ orbital describes the two step coupling of the CO orbitals to the metal sp states and the d states. Moreover, the degree of back donation is site dependent, i.e., its type and geometry match, such that the fourfold hollow sites provide better back donation than twofold bridging sites and atop sites in Ni(1 0 0) surface, but still worse than fcc hollow sites of Ni(1 1 1).

3.1.6. Adsorbed hydrogen atom

Previous studies of the atomic hydrogen adsorption on the Ni(1 0 0) surface [93,94] have shown that H prefers to the high-coordination site. Our GGA-DFT calculation gives the adsorption energy of 273 kJ/mol on the fourfold site, which is in well agreement with the result from Hammer et al. [95] 256 kJ/mol, and gives the normal distance of H to the surface of 0.596 versus his 0.60 Å, shown in Table 1. Also transmission channeling experiments, made by Stensgaard and Jakobsen [96], measured the adsorption height and yielded the experimental value of 0.50 ± 0.10 Å. Comparing the adsorption geometry of H on Ni(1 0 0) (see Fig. 2) with that on Ni(1 1 1) [66], we should found that although it is fourcoordinated on Ni(1 0 0), the longer H–Ni distance (1.859 Å on Ni(1 0 0) versus 1.699 Å on Ni(1 1 1)) may rationalize the difference in adsorption energies (273.43 on Ni(1 0 0) versus 284.32 kJ/mol on Ni(1 1 1)). By the way, Hafner also concluded that it has higher adsorption energy and longer $d_{H–Ni}$ of 1.81 Å on Ni(1 0 0) than that on Ni(1 1 1) surface [93].

3.1.7. Adsorbed hydroxymethyl

Theoretical studies of the thermochemistry [61,64] and kinetics [54,60] of the methanol decomposition have suggested that it proceeds through initial C–H bond scission to produce hydroxymethyl on some transition metals. And for its adsorption, density functional theory of cluster calculations [61,64] and periodic slab calculations [54,60] have indicated that the coordination via carbon is more favorable than via oxygen. Our calculated adsorption configuration for adsorption ($R_{CNi} = 1.925$ and $R_{ONi} = 2.061$ Å) on Ni(1 0 0) is in agreement with these studies (Fig. 2), and is also adsorbed at the top site as on Ni(1 1 1). Also the calculated adsorption energy and the R_{CNi} are 176.98 kJ/mol and 1.925 Å, which is higher and shorter than on Ni(1 1 1) surface (162.19 kJ/mol and 1.939 Å), as it should be.

Although, to our knowledge, no experimental structural information of CH_2OH/Ni and the activation energy barrier of methanol decomposition through C–H scission have been reported, it will be investigated in our future works including the mechanism of (M10*)–(M13*).

3.1.8. Adsorbed methyl

Based on the systematic investigation of the equilibrium geometry and the binding characteristics, we find methyl is preferably adsorbed on Ni(1 0 0) surface at the twofold hollow site (i.e., bridge site) with local C_{3v} symmetry, the molecular symmetry axis is nearly perpendicular to the surface with a very small tilting angle of 3.2° (Fig. 2). The adsorption energy is 184.14 kJ/mol, which is slightly higher than on the fourfold site, 177.72 kJ/mol, and is about 10 kJ/mol smaller than our previous calculation for CH_3 on Ni(1 1 1) [66]. Siegbahn and Panas [97] have carried out the bond prepared cluster calculations to model CH_3 adsorption on Ni(1 0 0) and Ni(1 1 1), and obtained the adsorption energy of 192 kJ/mol and 205 kJ/mol for the fourfold hollow site on Ni(1 0 0) and threefold hollow site on Ni(1 1 1), respectively. This energy difference is not large but it appears that there may be an actual difference between (1 0 0) and (1 1 1) caused by less optimal bond overlap at higher-coordination site on the Ni(1 0 0) surface. Upton have also studied methyl adsorption in the hollow site of Ni(1 0 0) and found a chemisorption energy of 280 kJ/mol by using a 20-atom cluster model and the GVB (generalized valance bond) method [56] The binding energies from both cluster calculations are significantly higher than our values. This discrepancy perhaps could be due to the finite cluster sizes and employing different computational methodology in those studies. In our most stable configuration, equilibrium height of carbon atom above the surface is 1.64 Å, and lower than 1.89 Å of Panas and co-workers [97], which is due to the difference of adsorption site despite of adsorbed on the same crystal surface. Compared with our height of CH_3 on Ni(1 1 1) [66], the higher value of distance to surface on Ni(1 0 0) also suggested that the H–metal interactions do not exist on Ni(1 0 0), unlike the case on Ni(1 1 1) where the interaction has been evidenced by the low or soft C–H frequencies [98,99].

3.1.9. Adsorbed hydroxyl

OH is also found as a component in the catalytically activated hydrogen–oxygen reaction or in the water–gas shift reactions. For the adsorption of OH on Ni(1 0 0) surface, the present optimized results show that OH stabilizes with its O–H axis nearly normal to the nickel surface and the oxygen pointing towards the fourfold hollow site, with an adsorption energy of 324.54 kJ/mol. The distance of O–Ni is 2.090 Å, which is longer than our previous results on Ni(1 1 1), 1.943 Å [66], while the adsorption energy is higher than on Ni(1 1 1), which may suggest the importance of coordination number and the more diffusive O 2p lone pair electrons orbital as mentioned before, and the importance of back donation from Ni 3d orbital to OH 1π anti-bonding orbital [100] (i.e., the geometry matching between adsorbate orbital and the surface site). Ab initio SCF calculations have been done for OH adsorbed on Ni_5(1 0 0), by Bauschlicher in a mainly qualitative study on the geometry and bonding of OH to nickel [101]. Calculated R_{ONi} are 3.41 and 2.04 Å for OH at atop and fourfold sites, respectively, which is consistent with our value.

3.2. Reaction path

Although the spectroscopic identification of surface-bound reaction intermediates provides evidence for the fundamental understanding of reaction mechanism governing the decomposition of methanol on many transition metal surfaces, the acquisition of data on kinetic parameters for elementary surface steps is important for a detailed understanding of heterogeneous catalysis. In this section, the energetics of the methanol decomposition on the Ni(1 0 0) surfaces will be discussed in terms of the elementary reaction steps in the surface mechanism, and compared with that on the Ni(1 1 1).

3.2.1. Surface dehydrogenation reactions

3.2.1.1. Hydrogen abstraction from methanol (M2). Cleavage of the O–H bond of methanol upon its adsorption on nickel metals appears to be a general phenomenon, occurring at low temperatures and leading to the formation of the stable methoxy intermediates [4,9–14], which have been shown by EELS [11], scanning kinetic spectroscopy (SKS) [18], time-resolved-EELS (TR-EELS) [4,19], optical second harmonic generation (SHG) [20], reflection adsorption infrared spectroscopy (RAIRS) and kinetic isotope effect (KIE) [21]. Here we analyze the reaction barrier of the first step of the methanol decomposition pathway through the O–H scission. The initial state of this pathway is the weak adsorbed methanol configuration described above (Fig. 2). The final state after O–H activation is the coadsorbed CH_3O and H species, chosen to be placed above two neighbor fcc hollow sites [51], which have previously been recognized and assigned as the most stable adsorbed sites. As the O–H bond is activated, as shown in Fig. 3, the hydrogen atom in hydroxyl group begins to move away from the methoxy, and then the C–O bond turns to normal to the surface. Transition state (Fig. 3(c)) is located following the nudged elastic band method, and the H atom is stretched much closer to the surface than that of initial state (1.36 Å versus 2.34 Å), which results in a much larger R_{OH} than that on Ni(1 1 1) (1.19 Å versus 1.008 Å). Considering the Fig. 3, we find that the structure of transition state obtained looks like the final state, which is in contrary to that on Ni(1 1 1), but the calculated energy barrier of this decomposition step is similar, 52.23 kJ/mol, only slightly higher than our previous work on Ni(1 1 1) [66]. By comparison with known experiments, Hall et al. reported an approximate energy barrier of 58 kJ/mol on Ni(1 1 1) in pulsed laser induced desorption technique assuming a pre-exponential factor of $1 \times 10^{-3}\ s^{-1}$ [9], in his later study he also suggested that the decomposition reaction is a self-poisoned reaction and obtained the energy barrier of $(38 + 17\theta_{CH_3O})$ kJ/mol on Ni(1 0 0) [10]. Similarly, Richter and Ho had obtained an activation energy of 33 kJ/mol for the formation of methoxy from chemisorbed methanol on Ni(1 1 0) by using temperature-programmed reaction spectroscopy, low energy electron diffraction and temperature-programmed electron energy loss spectroscopy [19]. In any cases, these experimental barrier energies on three different crystal surfaces are very similar and in good agreement with our calculated value.

3.2.1.2. Hydrogen abstraction from methoxy (M5). The reaction pathway for the abstraction of hydrogen from the adsorbed methoxy, leading to the adsorbed formaldehyde and hydrogen is identified to be the rate-limiting step in our calculations. The initial state is chosen to be the most stable adsorbed geometry of methoxy in Fig. 2, and the final state is composed of hydrogen

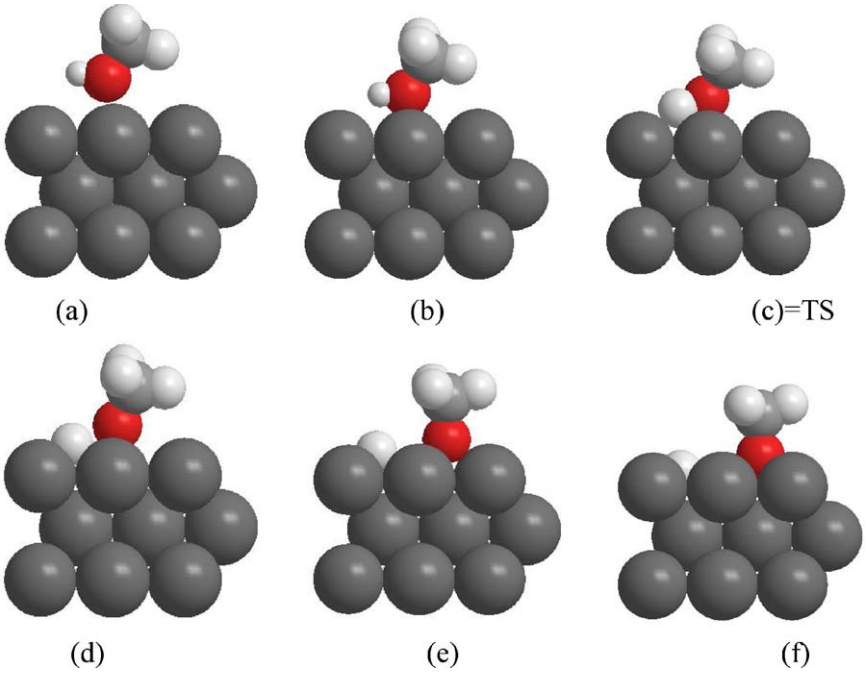

Fig. 3. Snapshots of the lowest energy reaction pathways identified for methanol dehydrogenation to CH_3O and H on Ni(1 0 0). Panel (a), the initial state, is the most stable adsorption structures of CH_3OH on Ni(1 0 0). Panel (c) illustrates the transition state for this process. Panel (f) is the final states of the reaction and correspond to the most stable coadsorptions of CH_3O and H within $p(3 \times 2)$ unit cells on Ni(1 0 0).

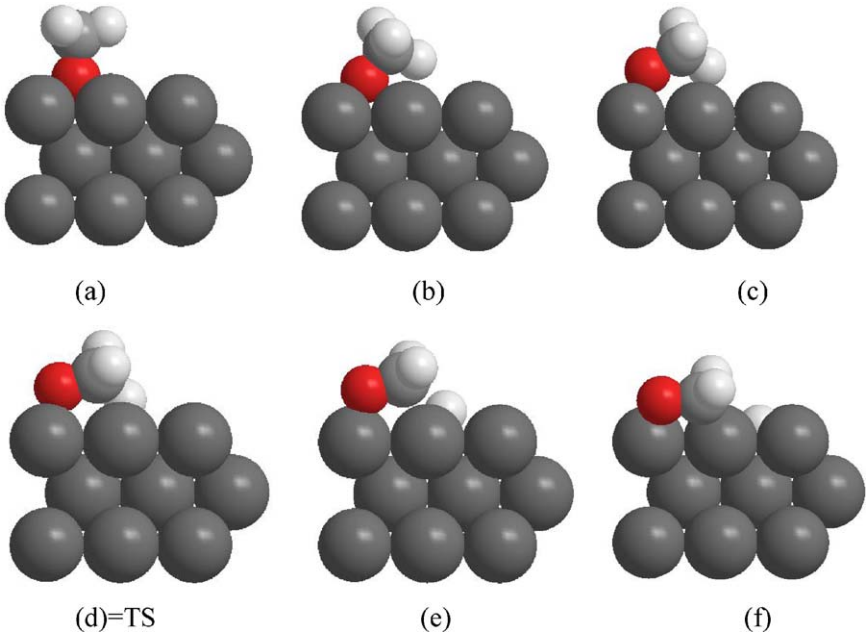

Fig. 4. Snapshots of the lowest energy reaction pathways identified for methoxy dehydrogenation to H_2CO and H on Ni(1 0 0): Panel (a), the initial state, is the most stable adsorption structures of CH_3O on Ni(1 0 0). Panel (d) illustrates the transition state for this process. Panel (f) is the final states of the reaction and correspond to the most stable coadsorptions of H_2CO and H within $p(3 \times 2)$ unit cells on Ni(1 0 0).

atom at fourfold site and formaldehyde in η^2 coordination geometry at top-bridged-top site. During a hydrogen atom abstracted from the initial normal methoxy state to its final hollow site, as show in Fig. 4, the C–O axis firstly tilts toward the surface and finally rotates to the most stable parallel configuration of adsorbed formaldehyde. In this process the hydrogen would be brought close enough to the surface through a proximal effect as suggested by Mutterties [102], which may be induced by the force forming bond between H–M, and resulting in the axis of the oxygen–carbon tilting to about 119° at the transition state. The structure of transition state in Fig. 4 is similar to that on Ni(1 1 1), i.e., formaldehyde-like. The activation energy calculated is the highest on Ni(1 0 0), 75.98 kJ/mol, and slightly lower than that of Ni(1 1 1). The reason can be interpreted with the BEP principle: the more stable the products, the lower the activation barrier (see the E_{ads} of CH_2O and H in Table 1), as illustrated in our previous work [66]. Also, the kinetics of methoxy decomposition reflects the competition between the strengthening of the M–O bond and the formation of M–H bond. The trend of H–M bond-making prevails over the O–M bond strengthening, resulting in the methoxy decomposition. In order to test effect of spin polarization and the surface-relaxation on the activation energy, an additional calculation with spin polarization and the surface-relaxation was made and the calculated value is 81.1 kJ/mol (see the data listed in Table 2), which is close to the un-relaxed model results.

The barrier we obtained is comparable to the results by experimental investigations. The experimental studies on Ni(1 1 1) and Ni(1 1 0) [103] have clearly demonstrated that cleavage of the C–H bond of methoxy to form surface-bound H_2CO species is the rate-limiting step. Barteau and co-workers find that the reaction barriers of methoxy decomposition has the same value of 70.6 kJ/mol on three surfaces of Ni(1 0 0), Ni(1 1 1), and Ni(1 1 0) [104]. In molecular beam experiments an activation

Table 2
DFT-GGA energetics data for possible elementary step in methanol decomposition over the Ni(1 0 0) surface

Step	ΔH_1[a]	ΔH_2[b]		Ea(f)	
	(1 0 0)	(1 0 0)	(1 1 1)	(1 0 0)	(1 1 1)
$CH_3OH = CH_3O + H$	435	−62.85	−54.26	52.23	39.46
$CH_3OH = CH_3 + OH$	385	−130.64	−102.01	177.28	169.87
$CH_3OH = CH_2OH + H$	393	−223.91	−1.21	87.48 (81.1)[c]	120.63
$CH_3O = H_2CO + H$	92	−32.77	7.68	75.98	85.95
$CH_2OH = H_2CO + H$	317	−80.24		86.76	
$H_2CO = HCO + H$	364	−50.57	−46.43	37.14	57.20
$HCO = CO + H$	71	−55.11	−129	76.0	17.0

Note: Energy in kJ/mol.

[a] ΔH_1 is the heat of reaction in the gas phase.

[b] ΔH_2 is the calculated heat of reaction on the surface based on the formula of $\Delta H_2 = E_{A+B} - E_{AB} \equiv Ea(f) - Ea(r)$.

[c] After the correlations of relax and spin effects.

energy for this step on nickel foil is believed to have been measured [44], and the reported value of 75 kJ/mol is consistent with our results. For the methoxy on Ni(1 1 1), very similar results have been obtained for the decomposition barrier energy, 71 ± 1.2 kJ/mol, by Hall et al. using optical second harmonic generation (SHG) [20]. As on Ni(1 0 0), Huberty and Madix find the activation energy of 70 ± 1.2 kJ/mol for methoxy decomposition to CO and hydrogen, by using time-resolved Fourier transform infrared spectroscopy (TR-FTIR), and assuming a first-order reaction [42]. With TPRS, LEED and TPEELS, the abstraction of the first hydrogen from methoxy is also found to be the rate-limiting step following a first-order kinetics, and an activation energy of 67 kJ/mol on Ni(1 1 0) is obtained [19]. From all of these findings, plus TPRS, LEED, TP-EELS and HREELS data on Ni(1 1 0) [4,19], the assumption that the decomposition of methoxy on Ni is not strongly structure-sensitive is supported.

3.2.1.3. Decomposition of formaldehyde to final product (M7) and (M8).* The interaction of formaldehyde with nickel metal surface is of obvious importance for controlling the reaction because experimentally H_2CO at different converages either decomposes or polymerizes quickly. The calculations indicate that although the formaldehyde has a rather high adsorption energy of 149.81 kJ/mol, which is much higher than its decomposition barrier energy, 37.14 kJ/mol (Table 2), indicating that formaldehyde with $\theta = 1/6$ ML easily decomposes, and supporting the experimental results. The decomposition begins with an C–H bond scission, and ends with the formyl and hydrogen species settling down at their most stable sites. As the C–H bond is broken, the H atom moves toward the nearest hollow site, while the remaining HCO group binds with nearly the same geometry as formaldehyde. The transition state is shown in Fig. 5(a), with the O–C bond length is 1.384 Å, suggesting an approximately divalent species, and the length of the C–H bond being broken is 1.341 Å, implying this is a product-like transition state. We also notice that the products are so strongly adsorbed, and that this is an exothermic step, with a heat of reaction, −50.57 kJ/mol, and the reaction barrier, 37.14 kJ/mol. As comparing with the corresponding data on Ni(1 1 1), the BEP principle is not likely violated.

Following the formaldehyde decomposition, the subsequent formyl decomposition into CO and atomic hydrogen over Ni(1 0 0) was found to has the activation energy of 76 kJ/mol (see Table 2 as well as Fig. 5(b)), which is higher as compared with the case of Ni(1 1 1), and it is also higher than the reaction of $H_2CO = HCO + H$ on Ni(1 0 0). The possible reason for the larger activation energy difference of HCO decomposition between (1 0 0) and (1 1 1) (i.e., 76 versus17 kJ/mol shown in Table 1) may be due to the much more stronger adsorption energy of HCO on Ni(1 0 0) than that on the Ni(1 1 1) (i.e., −303.68 against −232.17 kJ/mol in Table 1). After the production of adsorbed CO, since CO is very strongly bound to the nickel surface and the desorption of CO from Ni(1 0 0) is endothermic by 218.54 kJ/mol, and it is expected that the CO remains adsorbed and can become a poison for the further dehydrogenation of methanol.

3.2.2. Potential pathways of C–H and C–O bond scissions in methanol

Geometrical and energetical information for the most favorable configurations of methanol and of intermediates resulting from methanol decomposition through an initial O–H, C–H, and C–O bond scission on Ni(1 0 0) are given and discussed in Section 3.1. And each elementary step, resulting from methanol decomposition starting with O–H bond scission, together with the associated energetic information, are analyzed in Section 3.2.1. Now, the alternative pathways starting with C–H and C–O bond scission in methanol will be shown briefly below.

3.2.2.1. C–H bond scission (M3). From our calculations, the decomposition pathway via the C–H bond scission yields coadsorbed hydroxymethyl and hydrogen atom at their most stable site as described above. The dissociation process begins with the C–O axis tilting, and then the carbonic hydrogen approaches closer to the Ni(1 0 0) surface until the H atom touches the surface. The TS given in Fig. 5(c), with the C–H bond length elongating to 1.618 Å, the reaction barrier is 87.48 kJ/mol, which is about 12 kJ/mol higher than the energy barrier of the rate-limiting step of methoxy decomposition. In addition, we also calculated the activation barrier of the (M9*) step (i.e., $CH_2OH(a) = H_2CO(a) + H(a)$) and find the data is 86.76 kJ/mol(see Table 2), which is only a little higher than that of the rate-limiting step (M5). So it is believe that the methanol decomposition may be also involved C–H scission during a wide range of reaction conditions. On Ni wire the adsorbed CH_3OD formed monodeuterated formaldehyde, HDCO, but at some point of reaction this formula of HDCO may indicate the presence of an intermediate such as H–C–O–D (following (M10*)) [105]. Theoretically, this process has been investigated on Pt(1 1 1) surface with the thermochemistry [61,64] and kinetics [54,60] methods, although few experimental data were reported. The existence of the COD intermediate (following (M11*)) has been reported by Madix and co-workers [40] and produced through a fast subsequent dehydrogenation process from methyl group of methanol, which also by the way supports that this step (M11*) investigated here do exist. Because C–H bond scission may happen with the O–H bond scission pathway, the followed decomposition steps (asterisked) will be addressed in detail in another paper.

3.2.2.2. C–O bond scission (M4). Unlike the two initial possible pathways introduced above, the process of C–O bond scission very high activation energy, 177.28 kJ/mol, which may be owing to the more unstable coadsorption state of the decomposition products than the other ways, for the existing of a large direct repulsive interaction, arising from the very small distance (2.305 Å) between the methyl and hydroxyl, as shown in Fig. 5(d). In contrast, the pathways of methanol decomposition originating from O–H and C–H bond scissions always give rise to hydrogen atom as one of the product. Considering the initial state of the three pathways is exactly the same, therefore the difference among their reaction barriers only lies in the relative stability of the three TSs. As described above, in the TS of the O–H and C–H bond scission pathway, H locates at an off-top

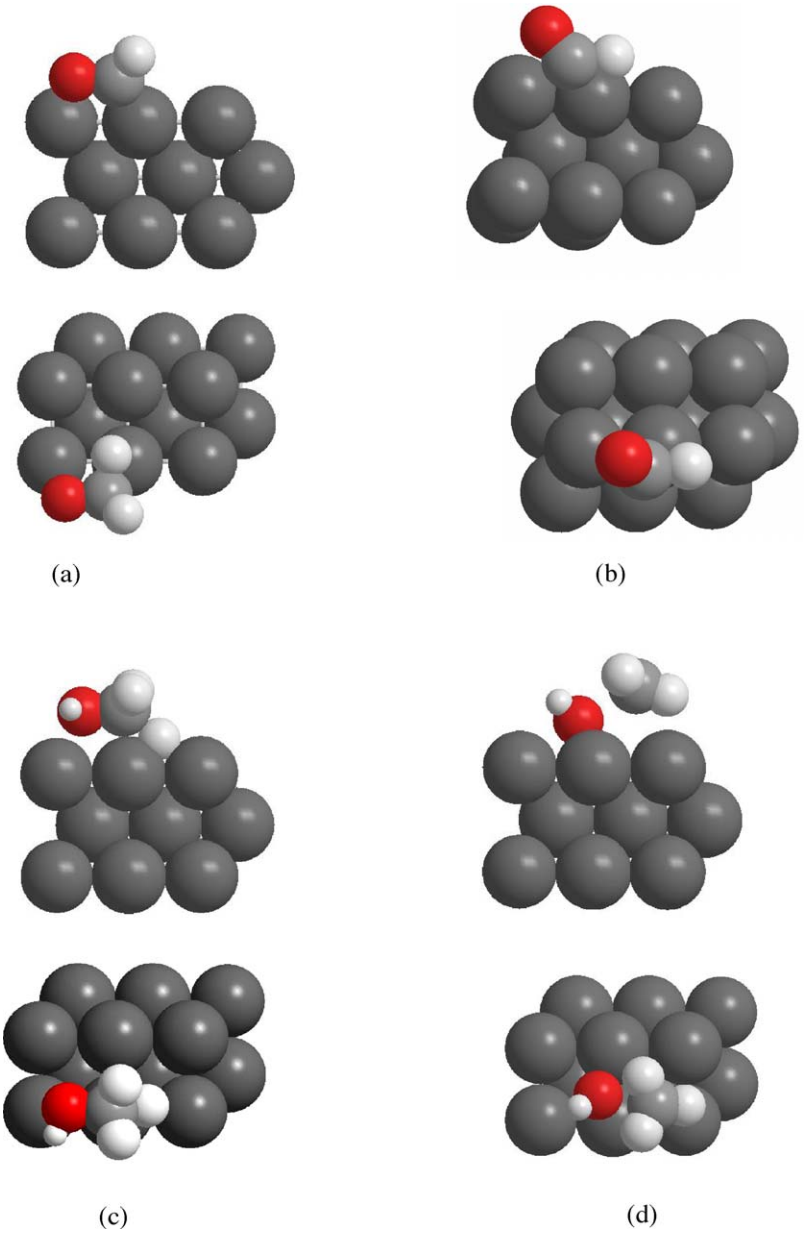

Fig. 5. Side view and top view of the configurations of the transition states during the decomposition H_2CO (a), decomposition of HCO (b), methanol initial with C–H (c) and C–O (d) bond scission.

site, while OCH_3 and CH_2OH site at close a bridge site, or at a close η^2 coordination site. However, in the TS configuration of the C–O bond scission pathway, although both the CH_3 and OH fragments need occupy a greater surface space, they are formed closer (R_{CO} 2.304 Å versus 2.325 Å) than on Ni(1 1 1). Apparently, a larger repulsive interaction will be occurred for the C–O broken, thus giving the highest barrier energy of decomposition.

Many catalytic reactions are structure-sensitive and the rate depends on the detailed geometrical structure of the surface atoms of the catalyst [106]. And the structure-sensitivity may reflect a variation in the intrinsic ability of the surface atoms to participate in surface chemistry, so it may be related to the surface openness, the coordination number of surface atoms, the geometry of adsorption sites, and the type of interaction or bonding between adsorbate–surface. For example, on copper surface, kinetic analysis has shown that the formate decomposition is a structure-sensitive reaction, and the reactivity following the order of Cu(1 1 1) > Cu(1 0 0) > Cu(1 1 0), while formate synthesis from CO_2/H_2 is a structure-insensitive reaction [107,108]. The structure-sensitivity has also been found in methanol synthesis, and the catalytic activity increases in the order of Cu(1 1 1) < Cu(1 0 0) < Cu(1 1 0) [109,110]. The difference of activity is considered to be due to the position of the neighboring Cu atoms. Based on the above calculation results (Table 2 and Fig. 6), it is reasonable to believe that the methanol decomposition on Ni metal may also a structure-sensitive reaction because of the activation energy difference of O–H bond broken and C–H bond broken in CH_3OH on Ni(1 0 0) and Ni(1 1 1) is so large which results in the larger difference in the productions. Similar phenomenon has also been observed

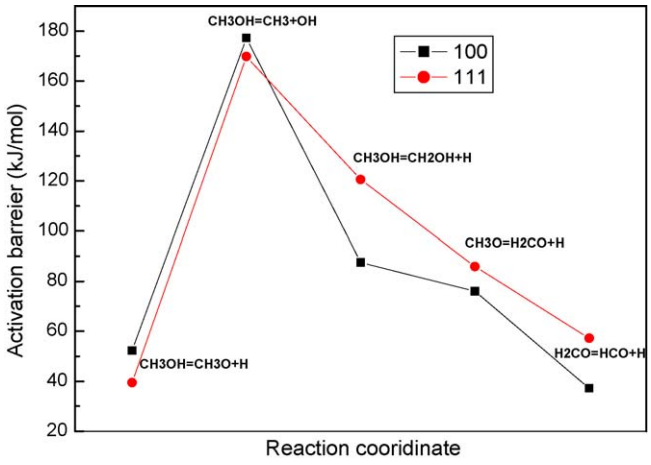

Fig. 6. Energy profile for the methanol decomposition on Ni(1 0 0) and Ni(1 1 1).

for the reaction of CH_3NH_2 decomposition in which the C–H bond broken of CH_3NH_2 occurred on Ni(1 1 1) and C–N bond broken appeared on Ni(1 0 0) [111].

4. Summary and conclusions

It is evident from our calculations that the decomposition via the O–H bond scission is much more energetically favorable than both the C–O bond scission and C–H bond scission. Compared with the previous work on Ni(1 1 1), the activation barrier difference between $CH_3OH(a) \rightarrow CH_2OH(a) + H(a)$ and $CH_3OH(a) \rightarrow CH_3O(a) + H(a)$ as well as $CH_3O(a) \rightarrow H_2CO(a) + H(a)$ and $CH_2OH(a) = H_2CO(a) + H(a)$ is much small on Ni(1 0 0), which indicates that both the O–H and C–H bond scission in methanol may be exist. However, barrier energy with C–O bond scission is in contrary, which may be due to the larger repulsive force between CH_3 and OH on Ni(1 0 0) than that on Ni(1 1 1). The rate-limiting step in methanol decomposition is the C–H scission of methoxy, and the end product of the pathway, CO, is shown to be so strongly bound that is could poison the Ni(1 0 0) surface. Above all, the mechanistic understanding emerging from the present work of examining methanol decomposition on Ni(1 0 0) differs from the previous studies on Ni(1 1 1), suggesting that the methanol decomposition on Ni (1 1 1) and Ni(1 0 0) might be a structure-sensitive reaction.

Acknowledgments

We wish to thank Doctors of Yoshitada Morikawa, Junji Nakamura and Professor of Zun-Sheng Cai for valuable discussion. This work was supported by the National Natural Science Foundation of China (Grants no. 20273034). This work was also partially supported by the NKStar HPC program and the Large Scale Numerical Simulation Project of Science Information Center, University of Tsukuba in Japan.

References

[1] G.v.d. Lee, V. Ponec, Catal. Rev. Sci. Eng. 29 (1987) 183.
[2] A.H. Jones, S. Poulston, R.A. Bennett, M. Bowker, Surf. Sci. 280 (1979) 31.
[3] F. Steinbach, R.J. Krall, J. Catal. 94 (1985) 142.
[4] L.J. Richter, B.A. Gurney, J.S. Villarrubia, W. Ho, Chem. Phys. Lett. 111 (1984) 185.
[5] R.J. Levis, Z.C. Jiang, N. Winograd, J. Am. Chem. Soc. 111 (1989) 4605.
[6] M. Endo, T. Matsumoto, J. Kubota, K. Domen, C. Hirose, Surf. Sci. 441 (1999) L931.
[7] J. Hrbek, R.A. de Paola, F.M. Hoffmann, J. Chem. Phys. 81 (1984) 2818.
[8] J.P. Lu, M. Albert, S.L. Bernasek, Surf. Sci. 239 (1990) 49.
[9] R.B. Hall, A.M. Desantolo, S.J. Bares, Surf. Sci. 137 (1984) 421–441.
[10] R.B. Hall, A.M. Desantolo, S.J. Bares, Surf. Sci. 161 (1985) L533.
[11] J.E. Demuth, H. Ibach, Chem. Phys. Lett. 60 (1979) 395.
[12] R.J. Madix, S.B. Lee, M. Thornburg, J. Vac. Sci. Technol. A 1 (1983) 1254.
[13] R.B. Hall, J. Phys. Chem. 91 (1987) 1007.
[14] R. Neubaure, C.M. Whelan, R. Denecke, H.-P. Steinruck, Surf. Sci. 507–510 (2002) 832.
[15] I. Nakabayashi, E. Nagao, K. Miyata, T. Moriga, T. Ashida, T. Tomida, M. Hyland, J. Metson, J. Mater. Chem. 5 (1995) 737.
[16] J.J. Vajo, J.H. Cambell, C.H. Becher, J. Phys. Chem. 95 (1991) 9457.
[17] J. Huberty, R.J. Madix, Surf. Sci. 360 (1996) 144.
[18] S.M. Gates, J.N. Russell Jr., J.T. Yates Jr., Surf. Sci. 159 (1985) 233.
[19] L.J. Richter, W. Ho, J. Chem. Phys. 83 (1985) 2569.
[20] R.B. Hall, A.M. DeSantlo, S.G. Grubb, J. Vac. Sci. Technol. A 5 (1987) 865.
[21] S.M. Gates, J.N. Russell Jr., J.T. Yates Jr., Surf. Sci. 146 (1984) 199.
[22] J.L. Erskine, A.M. Bradshaw, Chem. Phys. Lett. 72 (1980) 260.
[23] G.W. Rubloff, J.E. Demuth, J. Vac. Sci. Technol. 14 (1997) 419.
[24] C.M. Friend, X. Xu, Annu. Rev. Phys. Chem. 42 (1991) 251.
[25] I.E. Wachs, R.J. Madix, J. Catal. 53 (1978) 208.
[26] J.R.B. Gomes, J.A.N.F. Gomes, F. Illas, Surf. Sci. 443 (1999) 165.
[27] A.F. Carley, P.R. Davies, G.G. Mariotti, S. Read, Surf. Sci. 364 (1996) L525.
[28] C.H. Ammon, A. Bayer, G. Held, B. Richter, Surf. Sci. 507–510 (2002) 845.
[29] K. Amemiya, Y. Kitajima, Phys. Rev. B 59 (1999) 2307.
[30] M. Witko, K. Hermann, J. Chem. Phys. 101 (1994) 10173.
[31] H. Yang, J.L. Whitten, J.S. Huberty, R.J. Madix, Surf. Sci. 375 (1997) 268.
[32] H. Yang, J.L. Whitten, C.M. Friend, Surf. Sci. 313 (1994) 295.
[33] R. Zenobi, J. Xu, J.T. Yates Jr., B.N.J. Persson, A.I. Volokitin, Chem. Phys. Lett. 208 (1993) 414.
[34] M.A. Henderson, G.E. Mitchell, J.M. White, Surf. Sci. 188 (1987) 206.
[35] J.L. Davis, M.A. Barteau, J. Am. Chem. Soc. 111 (1989) 1782.
[36] L.J. Richer, W. Ho, J. Chem. Phys. 83 (1985) 2165.
[37] A.B. Anton, J.E. Parmeter, W.H. Weinberg, J. Am. Chem. Soc. 108 (1986) 1823.
[38] F.M. Leibsle, S.M. Francis, S. Haq, M. Bowker, Surf. Sci. 318 (1994) 46.
[39] I.E. Wachs, R.J. Madix, Surf. Sci. 76 (1978) 531.
[40] S. Johnson, R.J. Madix, Surf. Sci. 103 (1981) 361.
[41] F.L. Baudais, A.J. Borschke, J.D. Fedyk, M.J. Dignam, Surf Sci. 100 (1980) 210.
[42] J. Huberty, R.J. Madix, Surf. Sci. 334 (1995) 77.
[43] J. Miragliotta, R.S. Polizzotti, P. Rainowitz, S.D. Cameron, R.B. Hall, Chem. Phys. 143 (1990) 123–130.
[44] F. Steinbach, H.J. Spengler, Surf. Sci. 104 (1981) 318–340.
[45] H. Yang, J.L. Whitten, Langmuir 11 (1995) 853.
[46] D. Francoise, S. Philippe, Langmuir 9 (1993) 197.
[47] J.R.B. Gomes, W.A. Goddard III, S.P. Walch, A.K. Rappe, T.H. Upton, C.F. Melius, J. Vac. Sci. Technol. 14 (1997) 416.
[48] J.A.N.F. Gomes, F. Illas, J. Mol. Catal. A 170 (2001) 187.
[49] J.R.B. Gomes, J.A.N.F. Gomes, J. Mol. Struc. 503 (2000) 189.
[50] H. Yang, J.L. Whiitten, Surf. Sci. 313 (1994) 295.
[51] C.J. Zhang, P. Hu, J. Chem. Phys. 115 (2001) 7182.
[52] J. Greeley, M. Mavrikakis, J. Catal. 208 (2002) 291.
[53] J. Greeley, M. Mavrikakis, J. Am. Chem. Soc. 124 (2002) 7193.
[54] J. Greeley, M. Mavrikakis, J. Am. Chem. Soc. 126 (2004) 3910.

[55] P. Kratzer, B. Hammer, J.K. Norskov, J. Chem. Phys. 105 (1996) 5595.
[56] T.H. Upton, J. Vac. Sci. Technol. 20 (1982) 527.
[57] J.J. Chen, Z.C. Jiang, Y. Zhou, B.R. Chakraborty, N. Winograd, Surf. Sci. 328 (1995) 248.
[58] R.J. Levis, Z.C. Jiang, N. Winograd, J. Am. Chem. Soc. 110 (1988) 4431.
[59] N. Kruse, M. Reboholz, V. Matolin, G.K. Chuah, J.H. Block, Surf. Sci. Lett. 238 (1990) L457.
[60] K.D. Sanket, N. Matthew, K. Kourtakis, J. Phys. Chem. B 106 (2002) 2559.
[61] Y. Ishikawa, M. Liao, C.R. Cabrera, Surf. Sci. 463 (2000) 66.
[62] A. Michaelides, P. Hu, J. Am. Chem. Soc. 123 (2001) 4235.
[63] A. Alavi, P.J. Hu, T. Deutsch, P.L. Silvestrelli, J. Hutter, Phys. Rev. Lett. 80 (1998) 3650.
[64] J. Kua, W.A. Goddard, J. Am. Chem. Soc. 121 (1999) 10928.
[65] R.M. Watwe, B.E. Spiewak, R.D. Cortright, J.A. Dumesic, J. Catal. 180 (1998) 184.
[66] G.C. Wang, Y.H. Zhou, Y. Morikawa, J. Nakamura, Z.S. Cai, X.Z. Zhao, J. Phys. Chem. B 109 (2005) 12431.
[67] I.N. Remediakis, F. Abild-Pedersen, J.K. Nørskov, J. Phys. Chem. B 108 (2004) 14535.
[68] T. Hayashi, Y. Morikawa, H. Nozoye, J. Chem. Phys. 114 (2001) 7615.
[69] Y. Morikawa, K. Iwata, J. Nakamura, T. Fujitani, K. Terakura, Chem. Phys. Lett. 304 (1999) 91.
[70] Y. Morikawa, K. Iwata, K. Terakura, Appl. Surf. Sci. 169–170 (2001) 11.
[71] G.C. Wang, L. Jiang, Y. Morikawa, J. Nakamura, Z.S. Cai, Y.M. Pan, X.Z. Zhao, Surf. Sci. 570 (2004) 205.
[72] N. Troullier, J.L. Martins, Phys. Rev. B 43 (1991) 1993.
[73] G. Mills, H. Jónsson, G.K. Schenter, Surf. Sci. 324 (1995) 305.
[74] P. Maragakis, S.A. Andreev, G. Henkelman, B.P. Uberuaga, H. Jónsson, J. Chem. Phys. 113 (2000) 9901.
[75] G. Henkelman, H. Jónsson, J. Chem. Phys. 113 (2000) 9978.
[76] K. Brumer, D.R. Reichman, E. Kaxiras, J. Chem. Phys. 117 (2002) 4651.
[77] F. Mittendorfer, J. Hafner, J. Phys. Chem. B 106 (2002) 13299.
[78] F. Mittendorfer, J. Hafner, Surf. Sci. 472 (2001) 133.
[79] (a) G.C. Wang, Y.H. Zhou, J. Nakamura, J. Chem. Phys. 112 (2005) 044707;
(b) G.C. Wang, L. Jun, J. Comput. Chem. 26 (2005) 871.
[80] D.M. Newns, Phys. Rev. B 178 (1969) 1123.
[81] M.A. Henderson, Y. Zhou, J.M. White, J. Am. Chem. Soc. 111 (1998) 1185.
[82] C.J. Houtman, M.A. Barteau, J. Catal. 130 (1991) 528.
[83] B. Shekhar, M.A. Barteau, R.V. Plank, J.M. Vohs, J. Phys. Chem. B 101 (1997) 7939.
[84] F. Delbecq, P. Sautet, J. Catal. 211 (2002) 398.
[85] K. Sinniah, H.E. Dorsett, J.E. Reutt-Robey, J. Chem. Phys. 98 (1993) 9018.
[86] B. Hammer, Y. Morikawa, J.K. Nørskov, Phys. Rev. Lett. 76 (1996) 2141.
[87] B. Hammer, Phys. Rev. B 59 (1999) 7413.
[88] N. Vasquez Jr., A. Muscat, R.J. Madix, Surf. Sci. 339 (1995) 29.
[89] N. Vasquez Jr., A. Muscat, R.J. Madix, Surf. Sci. 301 (1994) 83.
[90] J.C. Bertolini, B. Tardy, Surf. Sci. 102 (1981) 131.
[91] W.A. Brown, R. Kose, D.A. King, Chem. Rev. 98 (1998) 797.
[92] G. Blyholder, J. Phys. Chem. 68 (1964) 2772.
[93] G. Kresse, J. Hafner, Surf. Sci. 459 (2000) 287.
[94] A. Grigo, D. Badt, H. Wengelnik, H. Neddermayer, Surf. Sci. 331–333 (1995) 1077.
[95] T.R. Mattsson, G. Wahnstrom, L. Bengtsson, B. Hammer, Phys. Rev. B 56 (1997) 2258.
[96] I. Stensgaard, F. Jakobsen, Phys. Rev. Lett. 54 (1995) 711.
[97] P.E.M. Siegbahn, I. Panas, Surf. Sci. 240 (1990) 37.
[98] M.B. Lee, Q.Y. Yang, S.L. Tang, S.T. Ceyer, J. Chem. Phys. 85 (1986) 1693.
[99] J. Robinson, D.P. Woodruff, Surf. Sci. 498 (2002) 203.
[100] H. Yang, J.L. Whitten, Surf. Sci. 223 (1989) 131.
[101] C.W. Bauschlicher Jr., Int. J. Quantum Chem. S20 (1986) 563.
[102] E.L. Mutterties, Chem. Soc. Rev. 11 (1982) 283.
[103] S.R. Bare, J.A. Stroscio, W. Ho, Surf. Sci. 150 (1985) 399.
[104] M. Mavrikakis, M.A. Barteau, J. Mol. Catal. A: Chem. 131 (1998) 35.
[105] M.W. Roberts, T.J. Stewart, in: Chemisorption and Catalysis, Pro. Conf. Inst. Petro., Ed. Pheeple, London, 1970, p. 16.
[106] M. Boudart, Adv. Catal. 20 (1996) 153.
[107] I. Nakamura, H. Nakao, T. Fujitani, T. Uchijima, J. Nakamura, J. Vac. Sci. Technol. A 17 (1999) 1592.
[108] T. Fujitani, Y. Choi, M. Sano, Y. Kushida, J. Nakamura, J. Phys. Chem. B 104 (2000) 1235.
[109] I. Nakamura, T. Fujitani, T. Uchijima, J. Nakamura, J. Vac. Sci. Technol. A 14 (1996) 1464.
[110] M.D. Crapper, C.E. Riley, D.P. Woodruff, A. Puschmann, J. Haase, Surf. Sci. 171 (1986) 1.
[111] C.C. Chang, C. Khong, S. Richard, J. Vac. Sci. Technol. 11 (1993) 2122.